Journal of Cellular and Molecular Medicine
A JOURNAL OF TRANSLATIONAL MEDICINE

J. Cell. Mol. Med. Vol 15, No 10, 2011 pp. 2150-2163

# γ-secretase complexes containing caspase-cleaved presenilin-1 increase intracellular Aβ42/Aβ40 ratio

**Louise Hedskog, Camilla A. Hansson Petersen, Annelie I. Svensson, Hedvig Welander, Lars O. Tjernberg, Helena Karlström, Maria Ankarcrona ***

*KI-Alzheimer's Disease Research Center, Karolinska Institutet, Department of Neurobiology, Care Sciences and Society (NVS), Stockholm, Sweden*

*Received: June 28, 2010; Accepted: September 28, 2010*

## Abstract

Markers for caspase activation and apoptosis have been shown in brains of Alzheimer's disease (AD) patients and AD-mouse models. In neurons, caspase activation is associated with elevated amyloid β-peptide (Aβ) production. Caspases cleave numerous substrates including presenilin-1 (PS1). The cleavage takes place in the large cytosolic loop of PS1-C-terminal fragment (PS1CTF), generating a truncated PS1CTF lacking half of the loop domain (caspCTF). The loop has been shown to possess important regulatory functions with regard to $A\beta_{40}$ and $A\beta_{42}$ production. Previously, we have demonstrated that γ-secretase complexes are active during apoptosis regardless of caspase cleavage in the PS1CTF-loop. Here, a PS1/PS2-knockout mouse blastocyst-derived cell line was used to establish stable or transient cell lines expressing either caspCTF or full-length CTF (wtCTF). We show that caspCTF restores γ-secretase activity and forms active γ-secretase complexes together with Nicastrin, Pen-2, Aph-1 and PS1-N-terminal fragment. Further, caspCTF containing γ-secretase complexes have a sustained capacity to cleave amyloid precursor protein (APP) and Notch, generating APP and Notch intracellular domain, respectively. However, when compared to wtCTF cells, caspCTF cells exhibit increased intracellular production of $A\beta_{42}$ accompanied by increased intracellular $A\beta_{42}/A\beta_{40}$ ratio without changing the Aβ secretion pattern. Similarly, induction of apoptosis in wtCTF cells generate a similar shift in intracellular Aβ pattern with increased $A\beta_{42}/A\beta_{40}$ ratio. In summary, we show that caspase cleavage of PS1 generates a γ-secretase complex that increases the intracellular $A\beta_{42}/A\beta_{40}$ ratio. This can have implications for AD pathogenesis and suggests caspase inhibitors as potential therapeutic agents.

**Keywords:** Alzheimer's disease • caspases • apoptosis • amyloid β-peptide • intracellular Aβ • $A\beta_{42}/A\beta_{40}$ ratio

## Introduction

Alzheimer's disease (AD) is a neurodegenerative disorder leading to progressive decline in memory and cognition. The hallmarks of AD pathology are extracellular deposits of amyloid β-peptide (Aβ) that aggregate into plaques [1] and intracellular deposition of hyperphosphorylated tau giving rise to neurofibrillary tangles [2]. Studies have demonstrated that intracellular accumulation of Aβ precedes extracellular deposits and may account for the initiating step in the pathogenesis causing neuronal and synaptic damage [3–5]. Furthermore, it has been suggested that intracellular accumulation of Aβ can form amyloid seeds that later will become extracellular plaques [6, 7]. Synaptic loss and neuronal dysfunction are early events in AD and occur before neuronal degeneration and plaque formation. In fact, the severity of the cognitive impairments correlates more strongly with synaptic loss and soluble Aβ levels than with amyloid plaque load [8, 9].

Aβ is generated from the amyloid precursor protein (APP) through sequential cleavage by β- and γ-secretases. The cleavage of APP by β-secretase generates two fragments; one extracellularly released soluble ectodomain (sAPPβ) and one membrane-anchored fragment (C99). The subsequent γ-secretase processing of C99 results in the generation of Aβ and the APP intracellular domain (AICD). γ-secretase determines the C-terminal of Aβ through cleavage of C99 in three steps, ε-, ζ- and γ-cleavage,

*Correspondence to: Maria ANKARCRONA,
KI-Alzheimer's Disease Research Center,
Karolinska Institutet, Department of Neurobiology,
Care Sciences and Society (NVS), Novum 5th Floor,
SE-141 86 Stockholm, Sweden.
Tel.: +46 8 58583617
Fax: +46 8 58583610
E-mail: Maria.Ankarcrona@ki.se

doi: 10.1111/j.1582-4934.2010.01208.x

generating Aβ of different lengths [10]. The two main forms are $A\beta_{40}$ and $A\beta_{42}$, the latter of which is the main constituent of amyloid plaques [11–14]. Several research groups have demonstrated that the relative level of $A\beta_{42}$ in relationship to $A\beta_{40}$ is critical for the pathogenesis of the disease, suggesting a central role of $A\beta_{42}$ in the development of AD [12, 15]. Furthermore, studies have shown that alterations in the $A\beta_{42}/A\beta_{40}$ ratio are important for Aβ toxicity and fibrillogenesis, and that $A\beta_{40}$-monomers could prevent aggregation and toxicity of $A\beta_{42}$ [16, 17]. γ-secretase is a multi-protein complex consisting of at least four subunits, including: presenilin 1 (PS1) or presenilin 2 (PS2), Nicastrin, anterior pharynx defective-1 (Aph-1) and presenilin enhancer-2 (Pen-2). Presenilin undergoes an endoproteolytic cleavage in its large cytosolic loop generating an N-terminal fragment (NTF) and a C-terminal fragment (CTF) (Fig. 2A). The two fragments form heterodimers in the γ-secretase complex, harbouring the two aspartic residues Asp257 and Asp385 that form the active site [18–20] (Fig. 2A). The large cytosolic loop in PS is believed to play an essential role in regulating the γ-secretase cleavage of APP at the γ-site which is responsible for the formation of Aβ species with different lengths [21, 22]. γ-secretase cleaves various type 1 transmembrane proteins, including APP, Notch and cadherins [23, 24]. There are numerous mutations in PS1 and PS2, which cause familial AD (FAD) (http://www.molgen.ua.ac.be/Admutations/). These mutations cause various phenotypes, including altered Aβ production [25–28], increased vulnerability to endoplasmatic reticulum stress [29, 30], disruption of intracellular $Ca^{2+}$ homeostasis [30, 31], disruption of neurotransmitter release [32, 33] and acceleration of apoptotic processes [34, 35].

Caspases, a group of cystein proteases cleaving after aspartyl residues, are activated by apoptotic stimuli and have been implicated in synaptic degeneration and neuronal loss in AD [36–38]. Several lines of evidence also suggest a correlation between caspase activation and elevated Aβ production [39–41]. Caspases cleave numerous substrates including APP, tau, PS1 and PS2. Recently, de Calignon and colleagues showed that caspase activation occurs before tangle formation *in vivo* in a Tg4510 mouse model and that caspase cleavage of tau is required for tangle formation [42]. Caspase cleavage of APP leads to the generation of two putative toxic peptides C31 and Jcasp [43]. However, Tesco *et al.* showed that the elevated Aβ production observed after caspase activation is independent of caspase cleavage of APP [39]. The role of presenilins in apoptosis has been studied by several groups showing that PS1 and PS2 in most cases accelerate the apoptotic program [44–48]. However, this may be dependent on the cell type since overexpression of PS1 (wild-type or FAD mutant) did not enhance apoptosis in cortical neurons [49]. Several caspases, including 1, 3, 6, 7, 8 and 11 have been shown to cleave PS1-CTF in the loop region at either Asp333 or Asp345 generating caspase cleaved CTF (caspCTF) (Fig. 2A) [50–52]. In contrast to CTFs and NTFs, caspase cleaved CTFs of PS1 and PS2 have been shown to delay anti-Fas induced apoptosis [53, 54]. Here we wanted to investigate whether γ-secretase complexes containing PSIcaspCTF give rise to altered Aβ production. We have previously shown that caspCTF, despite the truncation in the large cytosolic loop, forms active γ-secretase complexes in cells exposed to apoptotic stimuli [55]. In the present study we used a PS1/PS2 knockout mouse blastocyst-derived cell line (BD8), stably expressing PS1NTF and either stably or transiently expressing caspCTF starting at Ser346, or full length PS1CTF (wtCTF) starting at Ala299. We found that γ-secretase complexes containing PSIcaspCTF exhibited altered cleavage preference at the γ-site resulting in increased intracellular $A\beta_{42}/A\beta_{40}$ ratio.

**Table 1** Antibodies used in this study.

| Antibody | Name | Raised towards | Company/ gift from |
|---|---|---|---|
| NCT | N1660 | 693–709 | Sigma Aldrich |
| NCT | Nct | 168–289 | BD Bioscience (Sparks, MD, USA) |
| PS1-NTF | NT1 | N-terminal | Dr. Paul M Mathews |
| PS1-NTF | Ab14 | N-terminal 1–25 | Dr. Sam Gandy |
| Pen-2 | UD1 | N-terminal | Dr. Jan Näslund |
| Aph-1aL | ApH-1aL | C-terminal | Nordic Biosite (Täby, Sweden) |
| PS1-CTF | HZ-CTF | 455–467 | Dr. Hui Zheng |
| PS1-CTF | α-loopCTF | 263–378 | Chemicon Millipore (Billerica, MA, USA) |
| APP, C99/C83, Aβ | 6E10 | 1–16 | Convance (Princeton, NJ, USA) |
| βAPP, C99/C83, Aβ | 4G8 | 17–24 | Convance |
| βAPP | C1/6.1 | C-terminal | Dr. Paul M Mathews |
| NICD | Val1744 | Cleaved Notch1 between Gly1743 and Val1744 | Cell Signaling (Danvers, MA, USA) |
| GAPDH | MAB374 | | Chemicon Millipore |

NCT: nicastrin.

# Materials and methods

## Reagents

Staurosporine (STS) was purchased from Sigma Aldrich (St. Louis, MO, USA). The antibodies used are summarized (Table 1). Unless otherwise noted all growth medium, serum and reagents were purchased from Invitrogen (Lidingö, Sweden).

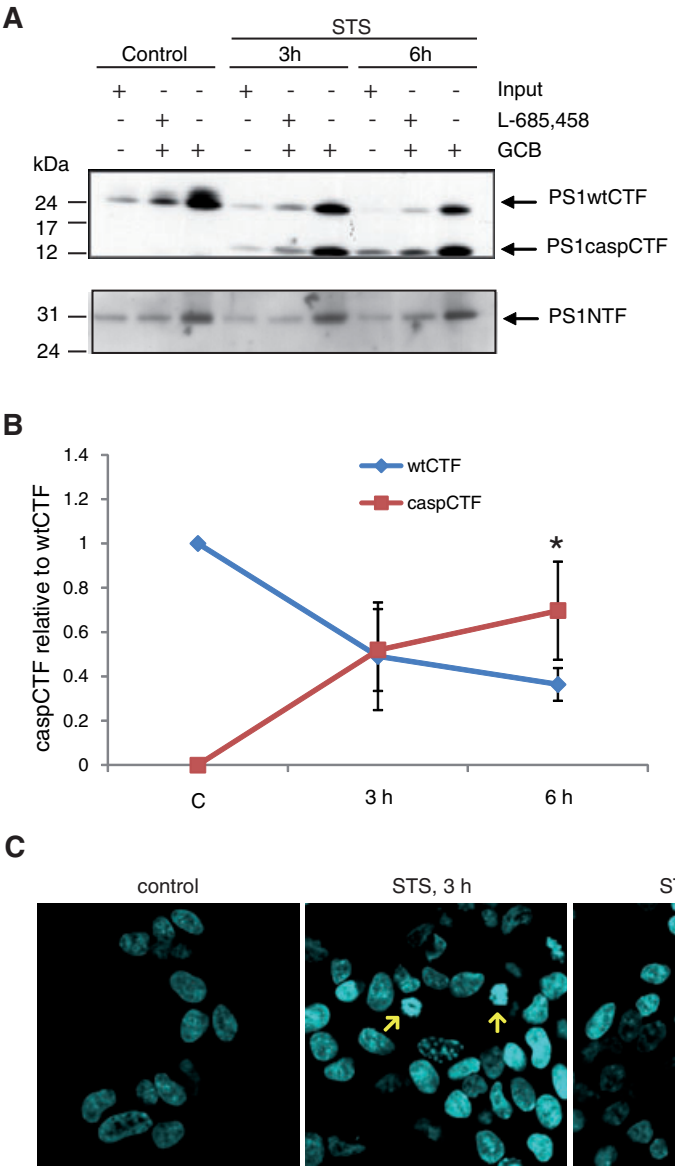


**Fig. 1** CaspCTF replace wtCTF in active γ-secretase complexes during apoptosis. SH-SY5Y-APP cells were exposed to STS (0.5 μM) for 3 or 6 hrs. (**A**) Active γ-secretase complexes were pulled down using GCB (200 nM) and streptavidin beads. As input, 8% of the lysate was used. To confirm specificity of the pulldown, we used a competitive non-biotinylated inhibitor L-685,458 (10μM). HZ-CTF antibody was used for detection of full-length CTF (PSIwtCTF) and caspase-cleaved CTF (PSIcaspCTF) by Western blot. Ab14 antibody was used for PS1NTF detection. (**B**) CCD-camera analysis of wtCTF and caspCTF band intensities in non-apoptotic cells (control) and in cells exposed to STS for 3 and 6 hrs (means ± S.D., *significant increase of caspCTF intensity as compared with wtCTF at $P < 0.05$ by Student's t-test, $N = 3$). (**C**) DAPI staining showing chromatin morphology in control and STS treated cells. Apoptotic cells are marked with arrows.

## cDNA constructs, cell culture and transfection

For the generation of stable cell lines, PS1wtCTF (starting at Ala-299) and PS1caspCTF (starting at Ser-346) were cloned into BglII and NotI sites of the pBudCE4.1 vector. C99 was thereafter cloned into HindIII and XbaI sites to generate the final constructs PS1wtCTFC99 and PS1caspCTFC99 (Fig. 1A). The CTF and NTF vectors used for transient transfection in the luciferase reporter gene assay have been described elsewhere [22]. All cDNA constructs were test-cleaved and sequenced for verification. Cells derived from $PS1^{-/-}$, $PS2^{-/-}$ mouse blastocysts (BD8 cells; lacking γ-secretase activity) [56] were cultured in Dulbecco's modified Eagle's medium (DMEM) supplemented with 10% (v/v) foetal bovine serum (FBS), 1 mM sodium pyruvate, 0.1 mM β-mercaptoethanol and non-essential amino acids. The BD8:PS1NTF cells (lacking PS2) were previously generated in our laboratory [57] and cultured in the same way as the BD8 cells but with a supplement of 1 μg/ml puromycin. The cDNA constructs were stably transfected into the BD8:PS1NTF cells using Lipofectamine Plus reagent according to the manufacturer's instructions. Single cell clones were generated by selection with 200 μg/ml Zeocine. A human neuroblastoma cell line, SH-SY5Y stably expressing human APP (a kind gift from Dr. Eirikur Benedikz, Karolinska Institutet, Stockholm, Sweden) was cultured in DMEM supplemented with 10% (v/v) FBS and 10 μM neomycin. All experiments were carried out in cells with a passage number less than 15, counted from the cloning time point.

## Characterization of established cell lines

For comprehensive analysis of the established cell lines, PCR analysis of genomic DNA and qRT-PCR analysis of mRNA levels were performed at

Bioinformatics and Expression Analysis, Department of Bioscience and Nutrition, Karolinska Institutet, Sweden. In brief, for PCR amplification of DNA extracted from wtCTF and caspCTF cell lines, the forward primers PEF-1$\alpha$ and the reverse primer BGHpA were used. The amplified products were separated by gel electrophoresis. For qRT-PCR analysis, the RNA extraction was done using RNeasy and then converted to cDNA with superscript III. The primers used were PS1-CTF-ANYF: TCATCGCTC TACACCTGAGTCA and PS1-CTF-ANYR: GTCTTCACCAGCGAGGATACTG. The probe 5′-FAM-CTGTCCAGGAACTTTC-3′ was designed by Applied Biosystems (Foster City, CA, USA). The mRNA was normalized to 18S rRNA.

To evaluate the protein expression in two wtCTF and two caspCTF clones the cells were harvested and homogenized with a high torque motor-driven pestle in 4-(2-hydroxyethyl)-1-piperazineethanesulfonic acid (HEPES)-lysis buffer: 20 mM HEPES (pH 7.5), 50 mM KCl, 2 mM ethylene glycol tetraacetic acid (EGTA) and protease inhibitor cocktail (Roche, Basel, Switzerland). Nuclei fraction was discharged and a membrane fraction collected after centrifugation at 100,000 $\times$ *g*. Membranes were resuspended and solubilized in radio-immunoprecipitation assay (RIPA)-buffert: 50 mM Tris (pH 7.5), 150 mM NaCl, 1% NP40, 0.5% deoxycholic acid, 0.1% SDS and protease inhibitor cocktail (Roche). After removal of cell debris, 10 and 30 $\mu$g cell lysate in Laemmli sample buffer (Sigma-Aldrich, Stockholm, Sweden) were subjected to SDS-PAGE.

## Western blot

Proteins were separated by SDS-PAGE using NuPAGE 4–12% Bis-Tris gels and nitrocellulose membrane (BioRad, Hercules, CA, USA). Membranes were incubated in Tris buffer saline–Tween 20 (0.1%) (TBS-T) + 5% milk for 30 min., followed by incubation with the primary antibody in TBS-T + 1% milk at 4°C over night on a shaking table. Membranes were rinsed three times in TBS-T and then incubated with the secondary antibody in TBS-T + 5% milk for 30 min. at room temperature. Finally membranes were washed three times in TBS-T and once in TBS before development. The immunoblots were visualized using Immobilon Western chemiluminescent horseradish perioxidase (HRP) substrate (Millipore Corporation, Billerica, MA, USA) and Amersham HyperfilmTM ECL (GE Healthcare, Uppsala, Sweden).

## Stability assay

wtCTF and caspCTF cells were cultured in six-well tissue-culture plates and exposed to 50 $\mu$g/ml cycloheximide for 0, 2, 4 and 6 hrs. Thereafter, the cells were washed in phosphate-buffered saline (PBS) and lysed in 200 $\mu$l whole cell extraction lysis buffer [20 mM HEPES pH 7.8, 0.42 M NaCl, 0.5% NP40, 25% glycerol, 0.2 mM ethylenediaminetetraacetic acid (EDTA), 1.5 mM $MgCl_2$, 1 mM ditiotreitol (DTT)] and protease inhibitor cocktail (Roche) for 30 min. at 4°C. After protein determination, 30 and 80 $\mu$g wtCTF and caspCTF cell lysates, respectively, were separated by SDS-PAGE and immunoblotted with HZ-CTF antibody. Glyceraldehyde 3-phosphate dehydrogenase (GADPH) and APP were used as negative and positive control, respectively. The band intensities ($N = 3$) were quantitatively measured using a CCD camera Las-3000 (Fuji film, Stockholm, Sweden).

## GCB pulldown

To investigate the levels of active $\gamma$-secretase complexes in the cell lines, the complexes were pulled down with a $\gamma$-secretase inhibitor coupled to biotin *via* a cleavable linker (GCB). GCB is designed in our laboratory and synthesized by Chemilia (Huddinge, Sweden). Details regarding GCB structure and characteristics have been published elsewhere [58]. Membrane fractions were prepared from two wtCTF and two caspCTF clones. The BD8 cells were used as a control. The membrane pellets were dissolved in 3-[(3-Cholamidopropyl) dimethylammonio]-2-hydroxy-1-propanesulfonate (CHAPSO) (1%) and after centrifugation at 10,000 $\times$ *g* the supernatant was incubated with GCB (200 nM). As input, 8% of the lysate was used. Streptavidin beads were used for pulldown. To confirm specificity of the pulldown we used a competitive non-biotinylated inhibitor L-685,458 (10 $\mu$M). Samples were subsequently separated on SDS-PAGE. For detection of the $\gamma$-secretase complex subunits by Western blot the following antibodies were used: N1660, HZ-CTF, NT1, UD1 and ApH-1aL (Table 1).

## Chromatin staining

SH-SY5Y-APP cells treated with STS (0.5 $\mu$M) for 3 and 6 hrs were fixed with 4% paraformaldehyde and stained with DAPI (4–6-diamidino-2-phenylindole) (Vector Laboratories, Burlingame, CA, USA). A LSM510 META confocal microscope (Carl Zeiss MicroImaging GmbH, Jena, Germany) was used to analyse the morphology of the chromatin.

## Activity assay measuring AICD and NICD production

Cells were harvested and homogenized in Buffer H: 20 mM Hepes (pH 7.4), 150 mM NaCl, 2 mM EDTA and protease inhibitor cocktail (Roche). The nuclei fraction was discharged and after centrifugation at 100,000 $\times$ *g* for 1 hr a membrane fraction collected. For AICD production, the membrane fraction was solubilized in Buffer H containing 1% CHAPSO and subsequently diluted to 0.4% CHAPSO. The membrane fraction was dissolved in pure Buffer H to produce NICD [59]. Unsolubilized membranes were removed by centrifugation at 10,000 $\times$ *g* for 5 min. Protein concentration was determined by BCA$^{TM}$ Protein Assay kit (Pierce, Rockford, IL, USA). For AICD production, the protein concentration was adjusted to 1 $\mu$g/$\mu$l and either incubated with dimethylsulfoxide (DMSO) (1:2000) or 1 $\mu$M $\gamma$-secretase inhibitor L-685,458 (Bachem Bioscience, Bubendorf, Switzerland) at 37°C for 16 hrs. The cleavage products were boiled and separated on 16% tricine gels, followed by Western blot analysis as described above. The AICD was detected with the monoclonal antibody C1/6.1 (Table 1). For NICD production, solubilized membranes were incubated at 37°C for 14 hrs and subsequently boiled and separated on 4–12% Bis-Tris gel. The Notch cleavage product, NICD was detected by Val1744 antibody (Table 1).

## Quantitative measurement of $\gamma$-secretase activity

The luciferase-based reporter gene assay was carried out as described previously [22, 60] with small modifications. In brief, once C99 is cleaved by $\gamma$-secretase, the AICD moiety fused to Gal4VP16 (GVP) migrates to the nucleus and activates the Gal4 response element fused to a luciferase reporter gene. BD8:PS1NTF cells cultured in 24-well plates, were transfected with total 550 ng DNA consisting of: 100 ng PS1wtCTFpcDNA5/caspCTFpcDNA5 or empty vector (pcDNA5), 200 ng MH100, 100 ng cytomegalovirus (CMV)-$\beta$-gal, 100 ng C99-GVP/N$\Delta$E-GVP and 50 ng GFP. Cells were lysed 48 hrs after transfection in 100 $\mu$l lysis buffer/well (10 mM Tris pH 8.1, 1 mM EDTA, 150 mM NaCl and 0.65% Igepal CA-630). Luciferase activity was measured after addition of luciferin and ATP (BioThema AB, Handen, Sweden). To normalize for transfection efficiency, $\beta$-galactosidase activity

was determined by absorbance reading at 405 nm in β-gal buffer (10 nM KCl, 60 mM $Na_2HPO_4$, 40 mM $NaH_2PO_4$, 1 mM $MgCl_2$, 50 μM β-mercaptoethanol and 8 mM *O*-nitrophenyl-β-D-galactopyranoside). Experiments were performed in triplicates and repeated four to six times.

## ELISA measurement of intracellular Aβ

ELISA was used to measure generated Aβ. wtCTF, caspCTF and BD8 cells ($1.5 \times 10^6$) were seeded and cultured in 2 × 10 cm dishes in 4 ml OptiMEM supplemented with 0.1% DMSO for 48 hrs. The BD8 cells were used as negative control (blank). Cells were subsequently exposed to normal or apoptotic conditions, induction of apoptosis was achieved by exposure to 0.1 μM STS for 6 hrs. In some experiments, the caspase inhibitor Z-VAD-FMK (Promega, Nacka, Sweden) 20 μM was added 30 min. before STS. Cells were then harvested in PBS and lysed in RIPA buffer. Detached cells floating in the media were spun down and pooled with harvested cells. The conditioned media was collected and saved for the procedure described below. Lysation was performed in a sonication water bath for 10 min., and thereafter on ice for 20 min. DMSO (0.38%) was added before the lysate was cleared by centrifugation at 4000 × *g* for 5 min. at 4°C. The ELISA plates used were human/rat β amyloid 40 ELISA kit II and Human/Rat β amyloid 42 ELISA kit Wako, High Sensitive (Wako Chemicals, Neuss, Germany). The ELISA measurements were performed according to the manufacturer's instructions. Standard curves were obtained using $Aβ_{40}$ and $Aβ_{42}$ peptides purchased from Bachem Bioscience, dissolved in HFIP (hexafluoroisopropanol) in a concentration of 1 mg/ml, sonicated for 30 min. and incubated in room temperature over night. The peptides were aliquoted to contain 100 μg/tube and the solvent was lyophilized under $N_2$ gas. Peptides were dissolved in DMSO in a concentration of 100 μM and stored in –80°C as 1 μl aliquots. Upon usage, the peptides were diluted in RIPA buffer. Triplicates were performed within each ELISA experiment.

## ELISA measurement of secreted Aβ

Simultaneously to intracellular Aβ measurement, we measured levels of $Aβ_{40}$ and $Aβ_{42}$ in conditioned media from the same cells as above exposed to normal or apoptotic conditions. The media was collected and 20% RIPA containing protease inhibitor cocktail was added. The standards were obtained using the above protocol except that OptiMEM supplemented with 20% RIPA buffer was used for the dilutions. Instead of colorimetric detection as above, a fluorescent detection method utilizing Amplex UltraRed Reagent (Invitrogen) was used to enhance the signal [61].

## Mass spectrometry

For detection of secreted Aβ in the cell lines, wtCTF, caspCTF and BD8 cells were cultured in OptiMEM for 48 hrs after which the media were collected. Amyloid-β residing in the media was immunoprecipitated using tosylactivated magnetic beads covalently coupled to 4G8 and 6E10 antibody (1:1) (Table 1) according to the manufacturer's instructions. The Aβ was eluted from the beads by vortexing for 2 min. in 0.5% formic acid (FA) and then dried by vacuum centrifugation (Maxi dry lyo; Heto, Allerød, Denmark). The samples were cleaved over night at 37°C in 80% FA with 1 mg of cyanogen bromide. Prior to liquid chromatography-mass spectrometry (LC-MS)/MS-analysis, the samples were concentrated and desalted using zip-tips (Millipore Corporation) according to the manufacturer's instructions, and subjected to vacuum centrifugation. The samples were subsequently dissolved in 0.1% FA and injected onto a 'high capacity enrichment column chip' with a 160 nl enrichment column, a 75 μm × 150 mm analytical column packed with Zorbax C18-SB 5 μm material (Agilent Technologies, Santa Clara, CA, USA). Peptides were eluted using a water/acetonitrile (ACN) gradient supplemented with 0.2% FA: from 2% to 14% ACN in 20 min. and 14–95% ACN in 20 min. The flow rate was 0.4 μl/min. delivered by an Agilent 1200 nano pump (Agilent Technologies). The column chip was coupled to an Agilent 6330 ion trap mass spectrometer (Agilent Technologies). Mass spectra were recorded from $m/z = 230$ to $m/z = 1800$. The monoisotopic masses for the Aβ fragments of interest were plotted as extracted ion chromatograms and MS/MS spectra confirmed the Aβ identity.

## Statistical analysis

In all experiments the nonparametric Mann-Whitney *U*-test was used to compare statistical differences between two groups ($n \geq 4$) with the exception of the first experiment in which active γ-secretase complexes containing caspCTF or wtCTF was compared. These data were transformed into t-distribution using log transformation before Student's t-test ($n = 3$) was applied. Values of $P < 0.05$ were considered to be significant.

# Results

## Caspase-cleaved CTF is part of active γ-secretase complexes

First, we studied caspase cleavage of active γ-secretase complexes during apoptosis. STS treatment is a well-established method to induce apoptosis both in a caspase-dependent and caspase-independent way [62]. Neuroblastoma cells, stably expressing human APP (SH-SY5Y-APP), were treated for 3 or 6 hrs with STS (0.5 μM). Active γ-secretase complexes were purified using GCB pulldown and then separated on SDS-PAGE. As a control for GCB specificity a γ-secretase inhibitor (L-685,458), which competes for binding to the active site, was used. In untreated cells, all of the PS1 containing γ-secretase complexes contained full length CTF (wtCTF) (Fig. 1A and B). After 3 hrs exposure to STS the γ-secretase complexes contained a ~50:50 mixture of wtCTF and caspCTF (Fig. 1A and B). After 6 hrs exposure the main constituent in active γ-secretase complexes was caspCTF (~65%). We employed DAPI staining to visualize apoptotic nuclei in STS treated cells (Fig. 1C). Lack of propidium iodide staining of non-fixated cells confirmed negligible induction of necrosis during STS treatment (data not shown). The results showed that caspCTF replaced wtCTF in active γ-secretase complexes during apoptosis.

## γ-secretase complexes containing caspCTF

In order to investigate the properties of γ-secretase complexes containing caspCTFs more carefully, we established stable cell

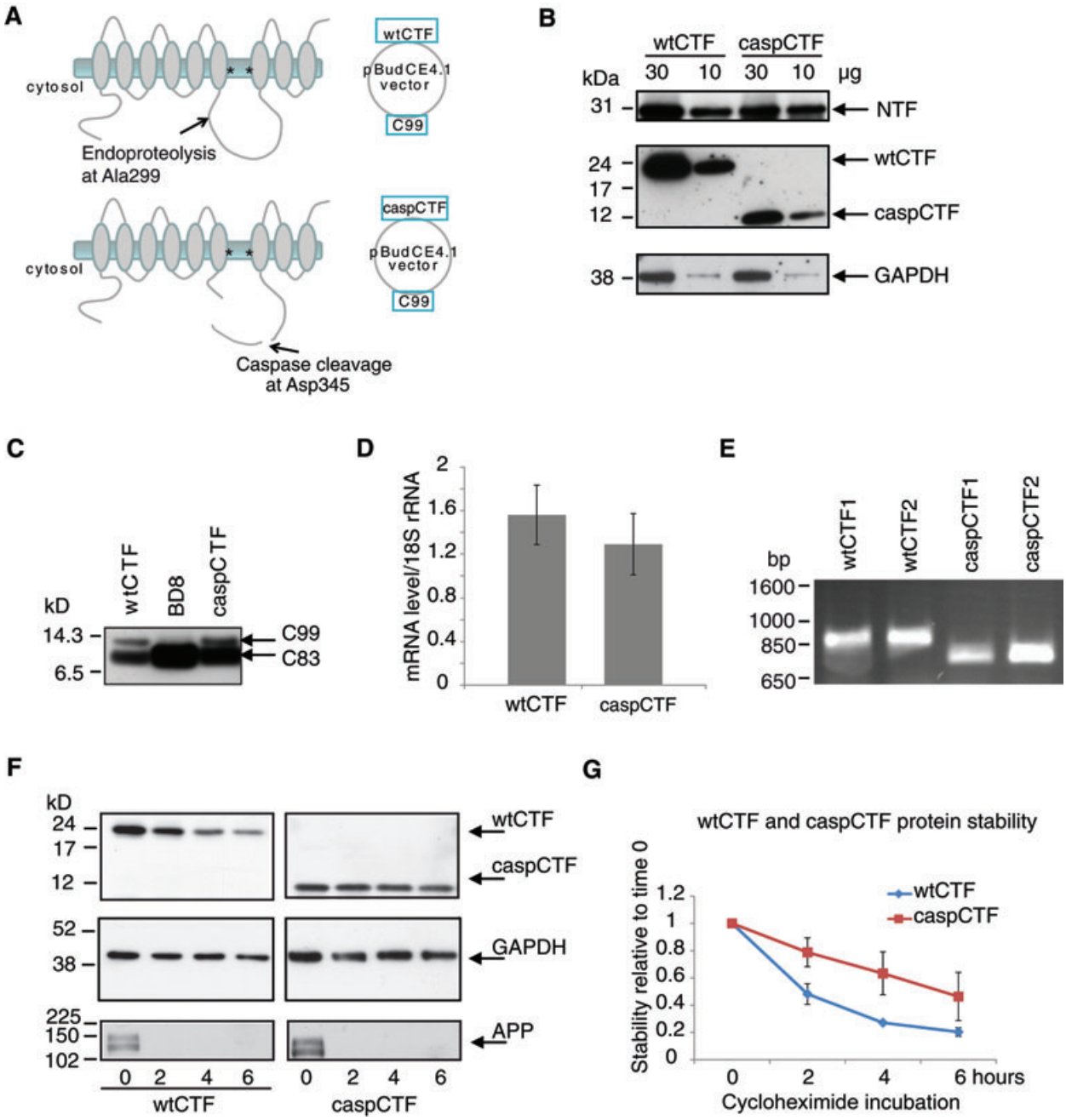


**Fig. 2** Design of vector constructs and characterization of the stable cell lines. (**A**) The catalytic site of the γ-secretase complex resides in TM6 and TM7 in PS, and is composed of D257 and D385, here represented by stars. PS undergoes endoproteolysis (A299) in the cytosolic loop generating NTF and CTF fragments. CTF can further be cleaved by caspases at position D345 or D333 resulting in a truncated membrane bound part. The final vector constructs contain either full length CTF (wtCTF) or caspase cleaved CTF at D345 (caspCTF) and both constructs contain C99. (**B**) Expression of NTF and wtCTF/caspCTF in membrane preparations from the cell lines. The molecular weight of wtCTF and caspCTF is 20 and 12 kD, respectively. GAPDH was used as loading control. (**C**) C99 and C83 expression. (**D**) qRT-PCR analysis of caspCTF and wtCTF mRNA. (**E**) PCR analysis of the genomic DNA in two wtCTF and in two caspCTF clones, the difference between full length CTF and caspCTF corresponds to the lack of 144 bp after caspase cleavage at D345. (**F**) Protein stability measurement of wtCTF and caspCTF using cycloheximide (50 μg/ml) exposure for 2, 4 and 6 hrs. GAPDH and APP were used as negative and positive controls, respectively. (**G**) CCD-camera band intensity analysis showing the stability over time (means ± S.D. of three independent experiments).

lines expressing C99 and either PS1caspCTF (starting at D345) or PS1wtCTF (starting at A299) on a BD8:PS1NTF background (Fig. 2A). For comparison of protein expression 10 and 30 μg of solubilized membrane preparation from wtCTF and caspCTF cell lines were analysed by Western blotting. The NTF expression was similar in both cell lines (Fig. 2B, upper panel). However, the expression of wtCTF was higher as compared to the expression of caspCTF (Fig. 2B, middle panel). Further, C99 expression was similar between the caspCTF and wtCTF cell lines (Fig. 2C). The BD8 cells (PS1/PS2 null) showed accumulation of C83 due to the lack of functional γ-secretase complexes. To study the expression levels of wtCTF and caspCTF in more detail we investigated the mRNA levels. As shown in (Fig. 2D), wtCTF and caspCTF cells displayed similar mRNA levels of wtCTF- and caspCTF-mRNA, respectively. Next we examined the size of wtCTF and caspCTF constructs by extracting genomic DNA from two clones from both caspCTF and wtCTF cell lines. Primers towards the vector were used and the amplified products were separated on a 0.7% agarose gel. The difference in size between wtCTF and caspCTF products appeared to be about 150 bp (Fig. 2E), which corresponded to the absence of 46 amino acids in the caspCTF construct. Next, we investigated the stability of caspCTF and wtCTF by inhibiting protein synthesis. To analyse the turnover time, adequate amounts of cell lysates (80 μg of caspCTF and 30 μg of wtCTF) were loaded and separated on SDS-PAGE. CCD-camera analysis was applied to measure the intensities of bands and revealed longer turnover time of caspCTF as compared to wtCTF after exposure to cycloheximide for 0, 2, 4 or 6 hrs (Fig. 2F and G). The turnover time of GAPDH and APP was used as negative and positive control, respectively.

To investigate if caspCTF forms active γ-secretase complexes, we compared the presence of active complexes in caspCTF and wtCTF cell lines by using two clones from each cell line. The active γ-secretase complexes were pulled down with GCB (Fig. 3A). An enrichment of γ-secretase components was obtained in the GCB pulldown as compared with the input, and the samples treated with L-685,458. All γ-secretase complex subunits, including Nicastrin, Aph-1, NTF, Pen-2 and full length CTF (20 kD), were detected in the wtCTF cells. These subunits were also found in the caspCTF cells, except for wtCTF (20 kD), which was substituted by caspCTF (12 kD). A comparison of the amount of subunits pulled down with GCB in each cell line, revealed that the caspCTF expressing cells contained fewer active γ-secretase complexes. Immature Nicastrin (the lower band) was detected in all lanes from all cell lines even in the control cell line (BD8) lacking both PS1 and PS2. However, mature Nicastrin (the higher band) was only detected in wtCTF and caspCTF cell lines and not in the BD8 cell line.

We further verified that the γ-secretase complexes were active by an *in vitro* activity assay detecting the formation of AICD and NICD. Solubilized membranes from wtCTF, caspCTF, BD8, SH-SY5Y and SH-SY5Y-APP were adjusted to contain equal amounts of protein and then incubated for 16 hrs at 37°C in the presence of γ-secretase inhibitor (L-685,458) or vehicle (DMSO). Both AICD and NICD production were found in caspCTF and wtCTF cell lines but not in the control cell line BD8 (Fig. 3B and C). For comparison, AICD formed by SH-SY5Y and SH-SY5Y-APP was loaded onto the same gel. However, the difference in amount of active γ-secretase complexes in the caspCTF and wtCTF cell lines made this method insufficient for quantitative measures between the cell lines.

## Intact cleavage at ε/S3-site in γ-secretase complexes containing caspCTF

To quantitatively investigate the activity of γ-secretase complexes containing caspCTF, we performed a luciferase-based reporter gene assay [60]. This method corrects for differences in transfection efficiency and is thereby suitable for enzymatic comparison. BD8:PS1NTF cells were transiently transfected with PS1wtCTF, PS1caspCTF or vehicle (empty pcDNA5 vector). Then the formation of AICD and NICD was measured with a luminometer and normalized to β-galactosidase activity. Similar AICD and NICD production was seen in caspCTF and wtCTF transfected cells, suggesting unchanged cleavage capacity at the ε/S3-site in γ-secretase complexes containing caspCTF (Fig. 4). Transfection with an empty pcDNA5 vector generated no AICD or NICD production (data not shown). Thus, γ-secretase complexes containing caspCTF had an unchanged capability of producing AICD and NICD as compared with γ-secretase complexes containing wtCTF.

## Caspase-cleaved CTF containing γ-secretase complexes exhibit altered Aβ production

Next, we analysed $A\beta_{40}$ and $A\beta_{42}$ levels in the caspCTF and wtCTF cells under apoptotic and non-apoptotic conditions. We found that the caspCTF cells displayed an altered intracellular Aβ production accompanied by an increased intracellular $A\beta_{42}/A\beta_{40}$ ratio (Fig. 5A and B). A statistical significance was found between the $A\beta_{42}/A\beta_{40}$ ratio in the caspCTF and the wtCTF expressing cells (Fig. 5B). The increased $A\beta_{42}/A\beta_{40}$ ratio in the caspCTF expressing cells raised the question whether induction of apoptosis in the wtCTF expressing cells could generate a similar shift in $A\beta_{42}/A\beta_{40}$ ratio. To investigate this, cells were subjected to 0.1 μM STS. Indeed, during apoptosis the intracellular $A\beta_{42}$ production as well as the $A\beta_{42}/A\beta_{40}$ ratio increased in the wtCTF cell line (Fig. 5A left panel and B). Interestingly, the combination of apoptosis and caspCTF-containing γ-secretase complexes generated an additive effect on $A\beta_{42}$ production in the caspCTF cells (Fig 5A, right panel) and, consequently, an even more elevated $A\beta_{42}/A\beta_{40}$ ratio (Fig. 5B). In parallel to intracellular measurements, we measured secreted Aβ in the conditioned medium. The results revealed that, during the conditions used here, neither apoptosis nor γ-secretase complexes containing caspCTF changed the secretion pattern (Fig. 5C and D). Next we investigated if the increase in intracellular $A\beta_{42}$ was caspase dependent by performing measurements in wtCTF and caspCTF cells co-treated with STS and the caspase inhibitor Z-VAD-FMK. As shown in (Fig. 5E, left panel), the elevation of $A\beta_{42}$ seen in wtCTF during apoptotic condition could be blocked with Z-VAD-FMK. Further, the formation of caspCTF-fragment during STS treatment was also blocked Z-VAD-FMK (Fig. 5E, lower panel). In the caspCTF cells, however, Z-VAD-FMK was not able to

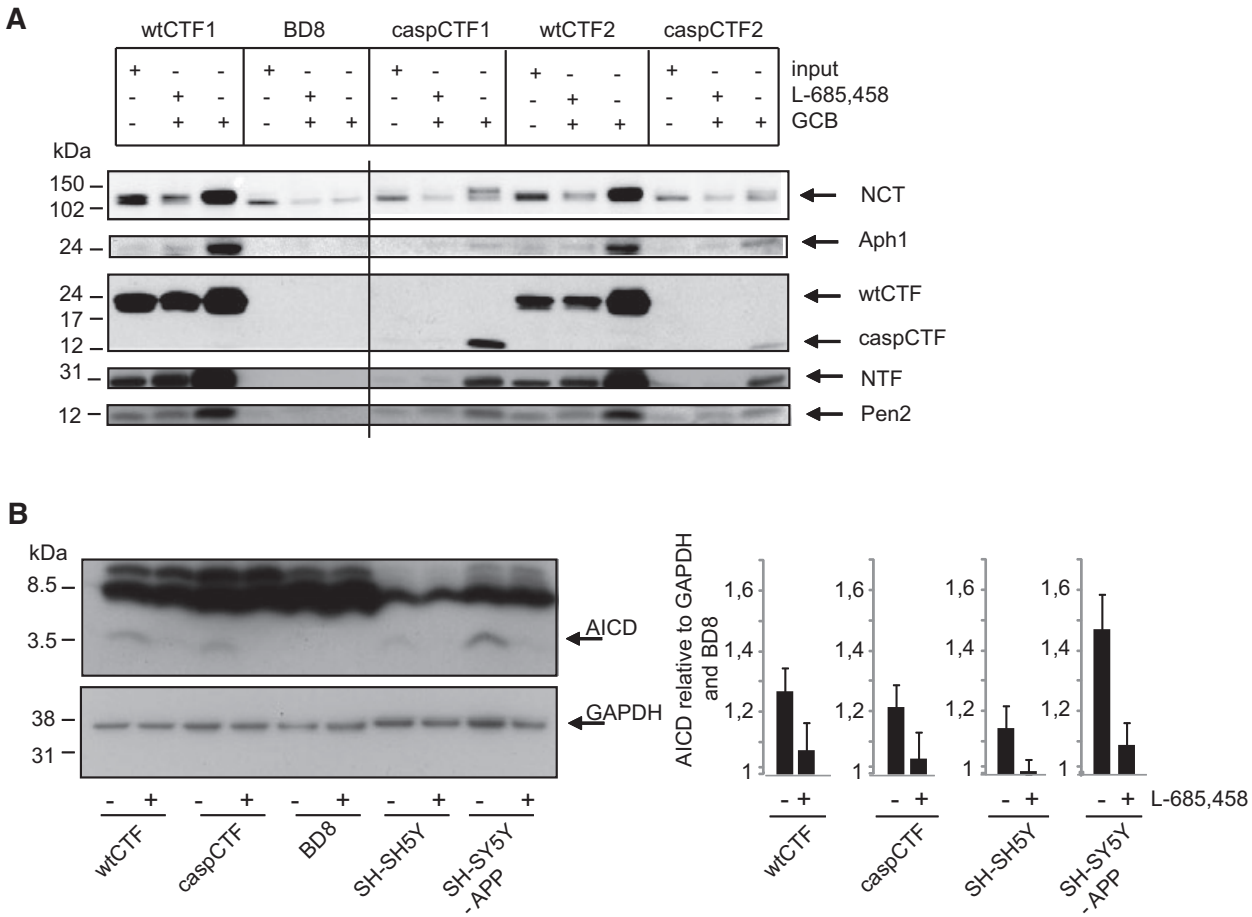


**Fig. 3** Characterization of γ-secretase complexes containing either caspCTF or wtCTF. (**A**) Active γ-secretase complexes were analysed by GCB pull down in two wtCTF and two caspCTF clones. BD8 cell line was used as control. Antibodies against Nicastrin (N1660), Aph-1 (Aph-1aL), PS1NTF (NT1), PS1CTF (HZ-CTF) and Pen-2 (UD-1) were used for detection of the γ-secretase subunits. (**B**) AICD production, in solubilized membranes from wtCTF, caspCTF, BD8, SH-SY5Y and SH-SY5Y-APP cells, was analysed after 16 hrs incubation at 37°C with vehicle (DMSO) or inhibitor (L-685,458). The antibody, C1/6.1, was used for detection of AICD. GAPDH was used as a loading control. The quantification is shown as AICD production normalized to GAPDH and BD8 ($N = 3$). (**C**) The cleavage product of Notch (NICD) was detected by Val1744 antibody.

block the elevation of $A\beta_{42}$ during STS induced apoptosis (Fig. 5E, right panel). BD8 cells were included in all ELISA experiments as a negative control and no Aβ production was detected in these cells (data not shown). Mass spectrometric analysis confirmed that both caspCTF and wtCTF expressing cells produced $A\beta_{42}$ while no production was detected in the BD8 cells (Fig. 5F). $A\beta_{40}$ could not be detected in this system due to low retention on the pre-column. In summary, we showed that γ-secretase complexes containing caspCTF exhibit an altered cleavage preference at the γ-site resulting in increased intracellular $A\beta_{42}/A\beta_{40}$ ratio without affecting the secretion pattern of $A\beta_{40}$ and $A\beta_{42}$.

## Discussion

In the present study, the relationship between caspase activation and elevated Aβ production was investigated. Activity of several

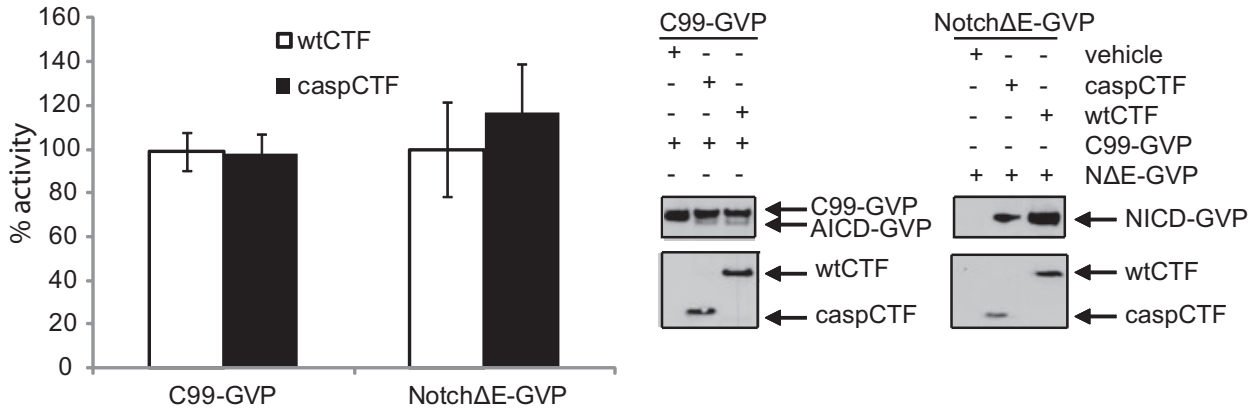


**Fig. 4** Quantitative measurement of γ-secretase activity in BD8:PS1NTF cells transiently expressing wtCTF, caspCTF or vehicle (empty pcDNA5 vector), together with C99-GVP/NotchΔE-GVP, MH100 and CMV-βgal constructs. The γ-secretase activity was determined using a luciferase-based reporter-gene assay, which monitors AICD and NICD production (means ± S.D. of ≥4 independent experiments, wtCTF was set to 100% activity for both AICD and NICD). Cell lysates subjected to SDS-PAGE (right panel). The antibody Val1744 was used for detection of S3 cleaved Notch-GVP and C1/6.1 used for AICD-GVP and C99-GVP. HZ-CTF antibody was used for detection of wtCTF and caspCTF.

caspases has been demonstrated in both postmortem brains as well as in the cerebrospinal fluid of sporadic and familial AD patients [37, 63–65]. Here, we studied γ-secretase complexes containing caspase-cleaved CTF (caspCTF) in two different cell lines, a neuroblastoma cell line (SH-SH5Y-APP) and a PS1/PS2 knockout mouse blastocyst-derived cell line (BD8:PS1NTF). Earlier studies have suggested that the cytosolic loop of PS is involved in regulating the enzymatic activity of the γ-secretase complex. This can for example be seen in cell lines on a PS deficient background [22], and in the absence of the entire loop in the PS1Δexon10 mouse model. These mice exhibited a great reduction of $A\beta_{40}$ but unchanged $A\beta_{42}$ levels accompanied by exacerbated plaque pathology [21]. Caspase cleavage at D345 in PS-loop region results in the loss of 46 amino acids corresponding to half the loop [50, 52]. Here, we found interesting differences in the Aβ profile between the stable cell lines expressing caspCTF and wtCTF indicating that this truncation also gives rise to altered Aβ production. Accordingly, we found that caspCTF cells had a significant increase in intracellular $A\beta_{42}/A\beta_{40}$ ratio as compared to wtCTF cells. These results indicate that caspase cleavage in the loop of PS1CTF changes the properties of the γ-secretase complex by altering its cleavage preference at the γ-site. Despite the truncation, the caspCTF cells exhibited similar production of AICD and NICD. Thus, the replacement of wtCTF by caspCTF in a γ-secretase complex does not affect the activity in regards to AICD and NICD production, although it has considerable impact on the cleavage at the γ-site. The precise biochemical mechanism underlying the resultant shift in Aβ production in the caspCTF-containing γ-secretase complexes is beyond the scope of this study. However, allosteric changes in PS1 conformation have been shown to underlie changes in the $A\beta_{42}/A\beta_{40}$ ratio [66]. We therefore speculate that the truncation in PS1 caused by caspase cleavage in the loop domain might alter the conformation in an $A\beta_{42}$ favouring fashion. This truncated γ-secretase complex may have implications in AD pathogenesis since it could be formed both early in and throughout the disease process as a result of caspase activation in affected brain regions. Furthermore, the longer turnover time of caspCTF as compared to wtCTF, as we have reported in this study, suggests that once it is formed it will be subjected to degradation in a lesser extent than wtCTF. Previous studies of caspCTFs have suggested a partly protective effect of these fragments due to their involvement in delaying anti-Fas induced apoptosis [53, 54]. During conditions of sustained caspase activation this effect may later be over-ridden by the accumulation of intracellular $A\beta_{42}$ as shown in the present study.

Interestingly, active caspases are also important for neuronal plasticity in the healthy brain, having a role in synaptic reorganization and neurite retraction [67]. Activation of caspases in synapses, neurites, and axon terminals causes local retraction or degeneration of the affected region without completion of the apoptotic program [68]. In fact, caspase activation in neurons can occur in a transient fashion and be important for long term depression [42, 69]. However, caspase activation and apoptosis have also been linked to synaptic loss and neurodegeneration in AD [40, 70–73]. In addition, Rohn *et al.* recently demonstrated an absence of pathology in the triple transgenic AD mice overexpressing anti-apoptotic protein Bcl-2 [74]. Several lines of evidence also suggest a correlation between caspase activation and elevated Aβ production [39, 41]. This elevation could partially be caused by up-regulation of APP and β-secretase (BACE), which has been detected during apoptosis [40, 75]. In addition, Aβ itself can trigger apoptotic cascades in neurons [76–79] and locally in synapses and dendrites [80]. Aβ aggregates have recently been shown to induce the extrinsic (caspase 8) apoptotic pathway while exposing cells to Aβ oligomers induced the intrinsic (caspase 9) apoptotic pathway [81]. Whether caspases or Aβ initiate neuronal

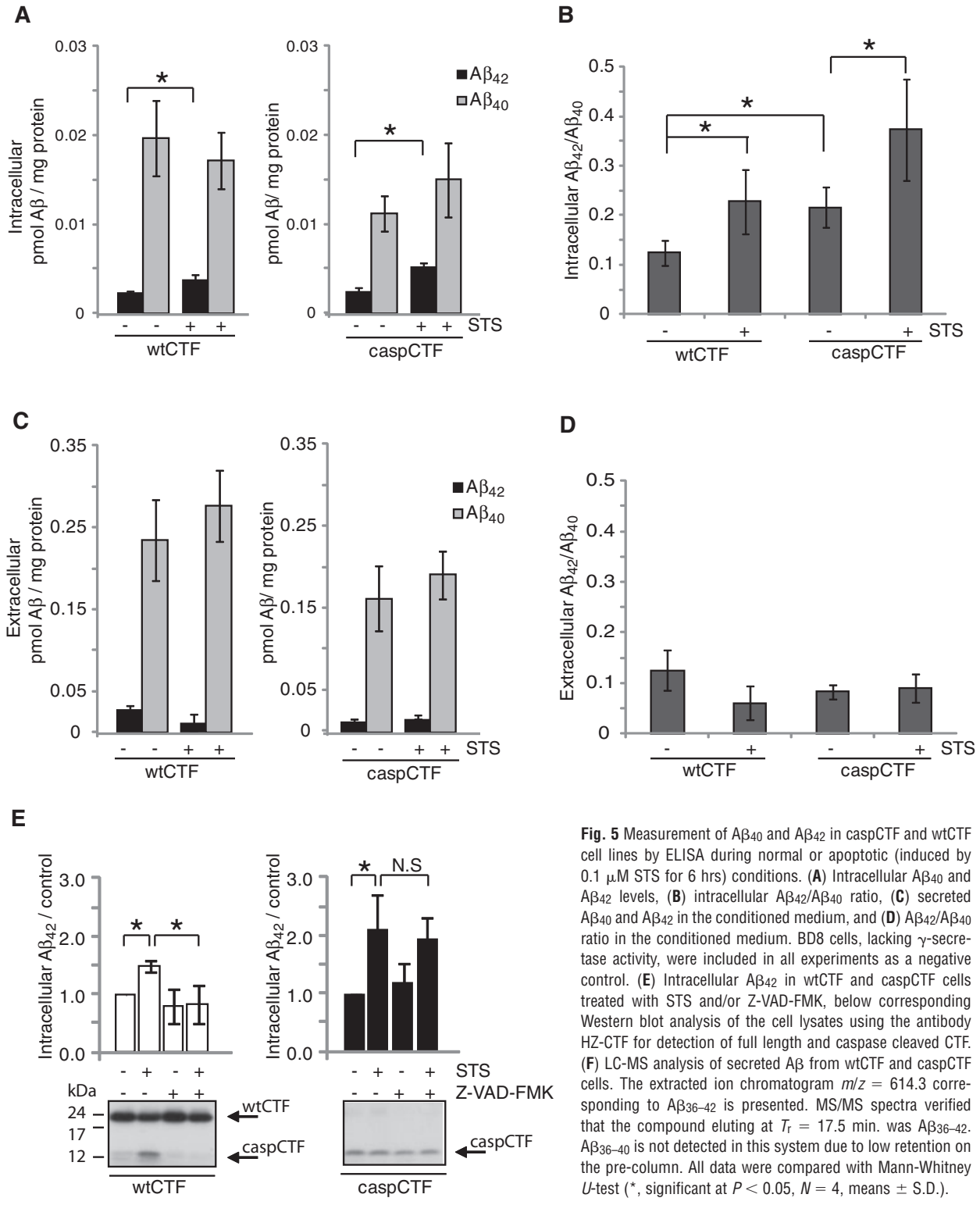


**Fig. 5** Measurement of $A\beta_{40}$ and $A\beta_{42}$ in caspCTF and wtCTF cell lines by ELISA during normal or apoptotic (induced by 0.1 μM STS for 6 hrs) conditions. (**A**) Intracellular $A\beta_{40}$ and $A\beta_{42}$ levels, (**B**) intracellular $A\beta_{42}/A\beta_{40}$ ratio, (**C**) secreted $A\beta_{40}$ and $A\beta_{42}$ in the conditioned medium, and (**D**) $A\beta_{42}/A\beta_{40}$ ratio in the conditioned medium. BD8 cells, lacking γ-secretase activity, were included in all experiments as a negative control. (**E**) Intracellular $A\beta_{42}$ in wtCTF and caspCTF cells treated with STS and/or Z-VAD-FMK, below corresponding Western blot analysis of the cell lysates using the antibody HZ-CTF for detection of full length and caspase cleaved CTF. (**F**) LC-MS analysis of secreted Aβ from wtCTF and caspCTF cells. The extracted ion chromatogram $m/z = 614.3$ corresponding to $A\beta_{36-42}$ is presented. MS/MS spectra verified that the compound eluting at $T_r = 17.5$ min. was $A\beta_{36-42}$. $A\beta_{36-40}$ is not detected in this system due to low retention on the pre-column. All data were compared with Mann-Whitney *U*-test (*, significant at $P < 0.05$, $N = 4$, means ± S.D.).

F

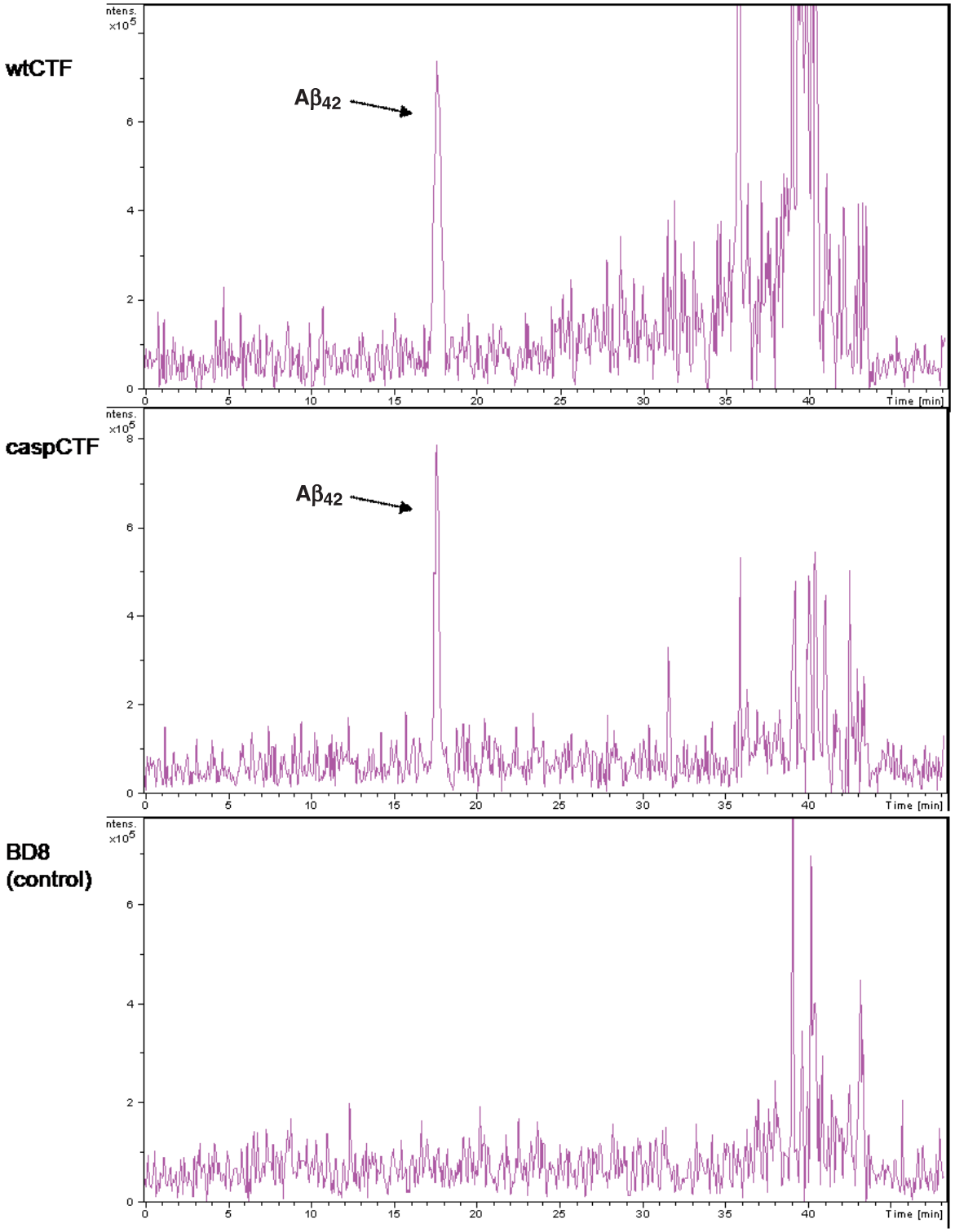


**Fig. 5** Continued.

degeneration is not known but the two events may cooperate in a vicious cycle.

The data from the caspCTF expressing cells showing increased intracellular $A\beta_{42}/A\beta_{40}$ ratio, was supported by additional experiments performed during apoptosis. Both increased intracellular $A\beta_{42}$ and elevated $A\beta_{42}/A\beta_{40}$ ratio were found in the wtCTF cells treated with STS for 6 hrs. Treatment with the caspase inhibitor Z-VAD-FMK diminished both the formation of caspase-cleaved CTF and the increase in intracellular $A\beta_{42}$. Thus, we demonstrate that during apoptosis γ-secretase complexes containing caspCTF are generated and will, at least in part, be responsible for the subsequent increase in intracellular $A\beta_{42}/A\beta_{40}$ ratio. Interestingly, in the caspCTF cells, whose γ-secretase complexes already exhibited altered cleavage preference in the γ-site, apoptotic stimuli prompted an additive intracellular increase in both $A\beta_{42}$ production and $A\beta_{42}/A\beta_{40}$ ratio. In contrast to the wtCTF cell line, this increase could not be blocked by Z-VAD-FMK, indicating the involvement of caspase independent pathways in this process. We speculate that morphological or biochemical alterations in the cell could generate conditions that alter APP processing in an $A\beta_{42}$ favouring manner for the caspCTF-containing γ-secretase complexes. Notably, no differences were observed between secreted $A\beta_{42}/A\beta_{40}$ ratios when comparing caspCTF with wtCTF cells during normal or apoptotic conditions. This suggests that the majority of $A\beta_{42}$ is retained inside the cells and that C99 processing, in our cell lines, does not primarily occur in the secretory pathway under the conditions used in our experiments. It is debated in which cellular compartment the γ-secretase complex exhibit its highest activity. Mitochondrial associated ER membranes for example have recently been suggested to contain enriched amounts of γ-secretase complexes [82], and it is possible that Aβ generated in such compartments remain intracellular.

In summary, since active caspases have been found in AD brain, the formation of γ-secretase complexes containing caspCTF reflects a scenario that could take place in the AD brain. Local activation of caspases in synapses could thereby shift the intracellular $A\beta_{42}/A\beta_{40}$ ratio and contribute to synaptic failure. The increased amounts of intracellular $A\beta_{42}$ could be neurotoxic, perhaps seed future amyloid plaques, and in this way contribute to AD pathogenesis. Our results suggest that caspase inhibitors may be worth investigating as potential therapeutic agents in AD.

## Acknowledgements

We thank Dr. Paul M. Mathews for the C1/6.1 and NT1 antibody, Dr. Sam Gandy for the Ab14 antibody and Dr. Hui Zheng for the HZ-CTF antibody. We are grateful to Dr. Jan Näslund for providing BD8:PS1NTF and to Dr. Eirikur Benedikz for the SH-SY5Y-APP cell line. We thank Michael Schöll for critically reading the manuscript. This work was supported by the Gun and Bertil Stohne's Foundation, Stiftelsen Gamla Tjänarinnor, Karolinska Institutet Belvén's Foundation, and Knut and Alice Wallenberg Foundation.

## Conflict of interest

The authors confirm that there are no conflicts of interest.

## References

1. **Hardy J, Selkoe DJ.** The amyloid hypothesis of Alzheimer's disease: progress and problems on the road to therapeutics. *Science*. 2002; 297: 353–6.
2. **Grundke-Iqbal I, Iqbal K, Tung YC, *et al.*** Abnormal phosphorylation of the microtubule-associated protein tau (tau) in Alzheimer cytoskeletal pathology. *Proc Natl Acad Sci USA*. 1986; 83: 4913–7.
3. **Wilson CA, Doms RW, Lee VM.** Intracellular APP processing and A beta production in Alzheimer disease. *J Neuropathol Exp Neurol*. 1999; 58: 787–94.
4. **Gouras GK, Tsai J, Naslund J, *et al.*** Intraneuronal Abeta42 accumulation in human brain. *Am J Pathol*. 2000; 156: 15–20.
5. **Aoki M, Volkmann I, Tjernberg LO, *et al.*** Amyloid beta-peptide levels in laser capture microdissected cornu ammonis 1 pyramidal neurons of Alzheimer's brain. *Neuroreport*. 2008; 19: 1085–9.
6. **D'Andrea MR, Nagele RG, Wang HY, *et al.*** Evidence that neurones accumulating amyloid can undergo lysis to form amyloid plaques in Alzheimer's disease. *Histopathology*. 2001; 38: 120–34.
7. **Hu X, Crick SL, Bu G, *et al.*** Amyloid seeds formed by cellular uptake, concentration, and aggregation of the amyloid-beta peptide. *Proc Natl Acad Sci USA*. 2009; 106: 20324–9.
8. **Terry RD.** Cell death or synaptic loss in Alzheimer disease. *J Neuropathol Exp Neurol*. 2000; 59: 1118–9.
9. **Terry RD, Masliah E, Salmon DP, *et al.*** Physical basis of cognitive alterations in Alzheimer's disease: synapse loss is the major correlate of cognitive impairment. *Ann Neurol*. 1991; 30: 572–80.
10. **Zhao G, Cui MZ, Mao G, *et al.*** Gamma-cleavage is dependent on zeta-cleavage during the proteolytic processing of amyloid precursor protein within its transmembrane domain. *J Biol Chem*. 2005; 280: 37689–97.
11. **Jarrett JT, Berger EP, Lansbury PT Jr.** The carboxy terminus of the beta amyloid protein is critical for the seeding of amyloid formation: implications for the pathogenesis of Alzheimer's disease. *Biochemistry*. 1993; 32: 4693–7.
12. **McGowan E, Pickford F, Kim J, *et al.*** Abeta42 is essential for parenchymal and vascular amyloid deposition in mice. *Neuron*. 2005; 47: 191–9.
13. **Welander H, Franberg J, Graff C, *et al.*** Abeta43 is more frequent than Abeta40 in amyloid plaque cores from Alzheimer disease brains. *J Neurochem*. 2009; 110: 697–706.
14. **Barrow CJ, Zagorski MG.** Solution structures of beta peptide and its constituent fragments: relation to amyloid deposition. *Science*. 1991; 253: 179–82.
15. **Kumar-Singh S, Theuns J, Van Broeck B, *et al.*** Mean age-of-onset of familial alzheimer disease caused by presenilin

mutations correlates with both increased Abeta42 and decreased Abeta40. *Human Mutat*. 2006; 27: 686–95.

16. **Jan A, Gokce O, Luthi-Carter R, *et al.*** The ratio of monomeric to aggregated forms of a{beta}40 and a{beta}42 is an important determinant of amyloid-{beta} aggregation, fibrillogenesis, and toxicity. *J Biol Chem*. 2008; 283: 28176–89.
17. **Yan Y, Wang C.** Abeta40 protects non-toxic Abeta42 monomer from aggregation. *J Mol Biol*. 2007; 369: 909–16.
18. **Wolfe MS, Xia W, Ostaszewski BL, *et al.*** Two transmembrane aspartates in presenilin-1 required for presenilin endoproteolysis and gamma-secretase activity. *Nature*. 1999; 398: 513–7.
19. **Leimer U, Lun K, Romig H, *et al.*** Zebrafish (Danio rerio) presenilin promotes aberrant amyloid beta-peptide production and requires a critical aspartate residue for its function in amyloidogenesis. *Biochemistry*. 1999; 38: 13602–9.
20. **Kimberly WT, Xia W, Rahmati T, *et al.*** The transmembrane aspartates in presenilin 1 and 2 are obligatory for gamma-secretase activity and amyloid beta-protein generation. *J Biol Chem*. 2000; 275: 3173–8.
21. **Deng Y, Tarassishin L, Kallhoff V, *et al.*** Deletion of presenilin 1 hydrophilic loop sequence leads to impaired gamma-secretase activity and exacerbated amyloid pathology. *J Neurosci*. 2006; 26: 3845–54.
22. **Wanngren J, Franberg J, Svensson AI, *et al.*** The large hydrophilic loop of presenilin 1 is important for regulating gamma-secretase complex assembly and dictating the amyloid beta peptide (Abeta) Profile without affecting Notch processing. *J Biol Chem*. 2009; 285: 8527–36.
23. **Wong PC, Zheng H, Chen H, *et al.*** Presenilin 1 is required for Notch1 and DII1 expression in the paraxial mesoderm. *Nature*. 1997; 387: 288–92.
24. **Baki L, Marambaud P, Efthimiopoulos S, *et al.*** Presenilin-1 binds cytoplasmic epithelial cadherin, inhibits cadherin/p120 association, and regulates stability and function of the cadherin/catenin adhesion complex. *Proc Natl Acad Sci USA*. 2001; 98: 2381–6.
25. **Takeda K, Araki W, Tabira T.** Enhanced generation of intracellular Abeta42 amyloid peptide by mutation of presenilins PS1 and PS2. *Eur J Neurosci*. 2004; 19: 258–64.
26. **Duff K, Eckman C, Zehr C, *et al.*** Increased amyloid-beta42(43) in brains of mice expressing mutant presenilin 1. *Nature*. 1996; 383: 710–3.
27. **Borchelt DR, Thinakaran G, Eckman CB, *et al.*** Familial Alzheimer's disease-linked presenilin 1 variants elevate Abeta1–42/1–40 ratio *in vitro* and *in vivo*. *Neuron*. 1996; 17: 1005–13.
28. **Ghidoni R, Albertini V, Squitti R, *et al.*** Novel T719P AbetaPP mutation unbalances the relative proportion of amyloid-beta peptides. *J Alzheimers Dis*. 2009; 18: 295–303.
29. **Katayama T, Imaizumi K, Manabe T, *et al.*** Induction of neuronal death by ER stress in Alzheimer's disease. *J Chem Neuroanat*. 2004; 28: 67–78.
30. **Zatti G, Burgo A, Giacomello M, *et al.*** Presenilin mutations linked to familial Alzheimer's disease reduce endoplasmic reticulum and Golgi apparatus calcium levels. *Cell Calcium*. 2006; 39: 539–50.
31. **Thinakaran G, Sisodia SS.** Presenilins and Alzheimer disease: the calcium conspiracy. *Nature Neurosci*. 2006; 9: 1354–5.
32. **Zhang C, Wu B, Beglopoulos V, *et al.*** Presenilins are essential for regulating neurotransmitter release. *Nature*. 2009; 460: 632–6.
33. **Parodi J, Sepulveda FJ, Roa J, *et al.*** Beta-amyloid causes depletion of synaptic vesicles leading to neurotransmission failure. *J Biol Chem*. 285: 2506–14.
34. **Miyoshi K, Ohyagi Y, Sakae N, *et al.*** Enhancement of activation of caspases by presenilin 1 gene mutations and its inhibition by secretase inhibitors. *J Alzheimers Dis*. 2009; 16: 551–64.
35. **McCarthy JV.** Involvement of presenilins in cell-survival signalling pathways. *Biochem Soc Trans*. 2005; 33: 568–72.
36. **Stadelmann C, Deckwerth TL, Srinivasan A, *et al.*** Activation of caspase-3 in single neurons and autophagic granules of granulovacuolar degeneration in Alzheimer's disease. Evidence for apoptotic cell death. *Am J Pathol*. 1999; 155: 1459–66.
37. **Albrecht S, Bogdanovic N, Ghetti B, *et al.*** Caspase-6 activation in familial alzheimer disease brains carrying amyloid precursor protein or presenilin i or presenilin II mutations. *J Neuropathol Exp Neurol*. 2009; 68: 1282–93.
38. **Louneva N, Cohen JW, Han LY, *et al.*** Caspase-3 is enriched in postsynaptic densities and increased in Alzheimer's disease. *Am J Pathol*. 2008; 173: 1488–95.
39. **Tesco G, Koh YH, Tanzi RE.** Caspase activation increases beta-amyloid generation independently of caspase cleavage of the beta-amyloid precursor protein (APP). *J Biol Chem*. 2003; 278: 46074–80.
40. **Xie Z, Dong Y, Maeda U, *et al.*** The inhalation anesthetic isoflurane induces a vicious cycle of apoptosis and amyloid beta-protein accumulation. *J Neurosci*. 2007; 27: 1247–54.
41. **Xie Z, Moir RD, Romano DM, *et al.*** Hypocapnia induces caspase-3 activation and increases Abeta production. *Neurodegenerat Dis*. 2004; 1: 29–37.
42. **de Calignon A, Fox LM, Pitstick R, *et al.*** Caspase activation precedes and leads to tangles. *Nature*. 2010; 464: 1201–4.
43. **Park SA, Shaked GM, Bredesen DE, *et al.*** Mechanism of cytotoxicity mediated by the C31 fragment of the amyloid precursor protein. *Biochem Biophys Res Commun*. 2009; 388: 450–5.
44. **Alves da Costa C, Mattson MP, Ancolio K, *et al.*** The C-terminal fragment of presenilin 2 triggers p53-mediated staurosporine-induced apoptosis, a function independent of the presenilinase-derived N-terminal counterpart. *J Biol Chem*. 2003; 278: 12064–9.
45. **Alves da Costa C, Paitel E, Mattson MP, *et al.*** Wild-type and mutated presenilins 2 trigger p53-dependent apoptosis and down-regulate presenilin 1 expression in HEK293 human cells and in murine neurons. *Proc Natl Acad Sci USA*. 2002; 99: 4043–8.
46. **Wolozin B, Iwasaki K, Vito P, *et al.*** Participation of presenilin 2 in apoptosis: enhanced basal activity conferred by an Alzheimer mutation. *Science*. 1996; 274: 1710–3.
47. **Cai C, Lin P, Cheung KH, *et al.*** The presenilin-2 loop peptide perturbs intracellular Ca2+ homeostasis and accelerates apoptosis. *J Biol Chem*. 2006; 281: 16649–55.
48. **Fluhrer R, Friedlein A, Haass C, *et al.*** Phosphorylation of presenilin 1 at the caspase recognition site regulates its proteolytic processing and the progression of apoptosis. *J Biol Chem*. 2004; 279: 1585–93.
49. **Bursztajn S, DeSouza R, McPhie DL, *et al.*** Overexpression in neurons of human presenilin-1 or a presenilin-1 familial Alzheimer disease mutant does not enhance apoptosis. *J Neurosci*. 1998; 18: 9790–9.
50. **Kim TW, Pettingell WH, Jung YK, *et al.*** Alternative cleavage of Alzheimer-associated presenilins during apoptosis by a caspase-3 family protease. *Science*. 1997; 277: 373–6.
51. **Grunberg J, Walter J, Loetscher H, *et al.*** Alzheimer's disease associated presenilin-1 holoprotein and its 18–20 kDa C-terminal fragment are death substrates for

proteases of the caspase family. *Biochemistry*. 1998; 37: 2263–70.

52. **van de Craen M, de Jonghe C, van den Brande I, *et al.*** Identification of caspases that cleave presenilin-1 and presenilin-2. Five presenilin-1 (PS1) mutations do not alter the sensitivity of PS1 to caspases. *FEBS Lett*. 1999; 445: 149–54.
53. **Vezina J, Tschopp C, Andersen E, *et al.*** Overexpression of a C-terminal fragment of presenilin 1 delays anti-Fas induced apoptosis in Jurkat cells. *Neurosci Lett*. 1999; 263: 65–8.
54. **Vito P, Ghayur T, D'Adamio L.** Generation of anti-apoptotic presenilin-2 polypeptides by alternative transcription, proteolysis, and caspase-3 cleavage. *J Biol Chem*. 1997; 272: 28315–20.
55. **Hansson CA, Popescu BO, Laudon H, *et al.*** Caspase cleaved presenilin-1 is part of active gamma-secretase complexes. *J Neurochem*. 2006; 97: 356–64.
56. **Donoviel DB, Hadjantonakis AK, Ikeda M, *et al.*** Mice lacking both presenilin genes exhibit early embryonic patterning defects. *Genes Dev*. 1999; 13: 2801–10.
57. **Bergman A, Laudon H, Winblad B, *et al.*** The extreme C terminus of presenilin 1 is essential for gamma-secretase complex assembly and activity. *J Biol Chem*. 2004; 279: 45564–72.
58. **Teranishi Y, Hur JY, Welander H, *et al.*** Affinity pulldown of gamma-secretase and associated proteins from human and rat brain. *J Cell Mol Med*. 2010; 14: 2675–86.
59. **Franberg J, Karlstrom H, Winblad B, *et al.*** Gamma-secretase dependent production of intracellular domains is reduced in adult compared to embryonic rat brain membranes. *PloS ONE*. 2010; 5: e9772.
60. **Karlstrom H, Bergman A, Lendahl U, *et al.*** A sensitive and quantitative assay for measuring cleavage of presenilin substrates. *J Biol Chem*. 2002; 277: 6763–6.
61. **Hashimoto M, Bogdanovic N, Volkmann I, *et al.*** Analysis of microdissected human neurons by a sensitive ELISA reveals a correlation between elevated intracellular concentrations of Abeta42 and Alzheimer's disease neuropathology. *Acta Neuropathol*. 2010; 119: 543–54.
62. **Belmokhtar CA, Hillion J, Segal-Bendirdjian E.** Staurosporine induces apoptosis through both caspase-dependent and caspase-independent mechanisms. *Oncogene*. 2001; 20: 3354–62.
63. **Louneva N, Cohen JW, Han LY, *et al.*** Caspase-3 is enriched in postsynaptic densities and increased in Alzheimer's disease. *Am J Pathol*. 2008; 173: 1488–95.
64. **Guo H, Albrecht S, Bourdeau M, *et al.*** Active caspase-6 and caspase-6-cleaved tau in neuropil threads, neuritic plaques, and neurofibrillary tangles of Alzheimer's disease. *Am J Pathol*. 2004; 165: 523–31.
65. **Albrecht P, Schmitz M, Otto M, *et al.*** Free caspase activity in CSF of patients with dementia. *J Neurol*. 2009; 256: 1561–2.
66. **Uemura K, Lill CM, Li X, *et al.*** Allosteric modulation of PS1/gamma-secretase conformation correlates with amyloid beta(42/40) ratio. *PloS ONE*. 2009; 4: e7893.
67. **Gilman CP, Mattson MP.** Do apoptotic mechanisms regulate synaptic plasticity and growth-cone motility? *Neuromol Med*. 2002; 2: 197–214.
68. **Mattson MP, Keller JN, Begley JG.** Evidence for synaptic apoptosis. *Exp Neurol*. 1998; 153: 35–48.
69. **Li Z, Jo J, Jia JM, *et al.*** Caspase-3 activation *via* mitochondria is required for long-term depression and AMPA receptor internalization. *Cell*. 141: 859–71.
70. **Galli C, Piccini A, Ciotti MT, *et al.*** Increased amyloidogenic secretion in cerebellar granule cells undergoing apoptosis. *Proc Natl Acad Sci USA*. 1998; 95: 1247–52.
71. **LeBlanc A.** Increased production of 4 kDa amyloid beta peptide in serum deprived human primary neuron cultures: possible involvement of apoptosis. *J Neurosci*. 1995; 15: 7837–46.
72. **Cicconi S, Gentile A, Ciotti MT, *et al.*** Apoptotic death induces Abeta production and fibril formation to a much larger extent than necrotic-like death in CGNs. *J Alzheimers Dis*. 2007; 12: 211–20.
73. **Takuma K, Yan SS, Stern DM, *et al.*** Mitochondrial dysfunction, endoplasmic reticulum stress, and apoptosis in Alzheimer's disease. *J Pharmacol Sci*. 2005; 97: 312–6.
74. **Rohn TT, Vyas V, Hernandez-Estrada T, *et al.*** Lack of pathology in a triple transgenic mouse model of Alzheimer's disease after overexpression of the anti-apoptotic protein Bcl-2. *J Neurosci*. 2008; 28: 3051–9.
75. **Nishimura I, Takazaki R, Kuwako K, *et al.*** Upregulation and antiapoptotic role of endogenous Alzheimer amyloid precursor protein in dorsal root ganglion neurons. *Exp Cell Res*. 2003; 286: 241–51.
76. **Nelson TJ, Alkon DL.** Protection against beta-amyloid-induced apoptosis by peptides interacting with beta-amyloid. *J Biol Chem*. 2007; 282: 31238–49.
77. **Loo DT, Copani A, Pike CJ, *et al.*** Apoptosis is induced by beta-amyloid in cultured central nervous system neurons. *Proc Natl Acad Sci USA*. 1993; 90: 7951–5.
78. **Yankner BA, Duffy LK, Kirschner DA.** Neurotrophic and neurotoxic effects of amyloid beta protein: reversal by tachykinin neuropeptides. *Science*. 1990; 250: 279–82.
79. **Zhang Y, McLaughlin R, Goodyer C, *et al.*** Selective cytotoxicity of intracellular amyloid beta peptide1–42 through p53 and Bax in cultured primary human neurons. *J Cell Biol*. 2002; 156: 519–29.
80. **Mattson MP, Partin J, Begley JG.** Amyloid beta-peptide induces apoptosis-related events in synapses and dendrites. *Brain Res*. 1998; 807: 167–76.
81. **Picone P, Carrotta R, Montana G, *et al.*** Abeta oligomers and fibrillar aggregates induce different apoptotic pathways in LAN5 neuroblastoma cell cultures. *Biophys J*. 2009; 96: 4200–11.
82. **Area-Gomez E, de Groof AJ, Boldogh I, *et al.*** Presenilins are enriched in endoplasmic reticulum membranes associated with mitochondria. *Am J Pathol*. 2009; 175: 1810–6.